

## Supporting Information

### Optimizing Sodium Storage and Durability in Metal Sulfide Anodes with 3D Graphene Architecture

Mujtaba Aminu Muhammad<sup>a</sup>, Yangjie Liu<sup>a</sup>, Baffa Haruna<sup>b</sup>, Ahmed Abdel-aziz<sup>a,b</sup>, Zul Qarnain<sup>b</sup>,  
Amir Mahmoud Makin<sup>b</sup>, Jiaqi Yu<sup>a</sup>, Zheng Bo<sup>c</sup>, Xiang Hu,<sup>a,\*</sup> Zhenhai Wen<sup>a,\*</sup>

<sup>a</sup> CAS Key Laboratory of Design and Assembly of Functional Nanostructures, and Fujian Provincial Key Laboratory of Materials and Techniques toward Hydrogen Energy, Fujian Institute of Research on the Structure of Matter, Chinese Academy of Sciences, Fuzhou, Fujian, 350002, China.

<sup>b</sup> University of Chinese Academy of Sciences, Beijing 100049, China.

<sup>c</sup> State Key Laboratory of Clean Energy Utilization, Zhejiang University

\* Corresponding authors: huxiang@fjirsm.ac.cn; wen@fjirsm.ac.cn

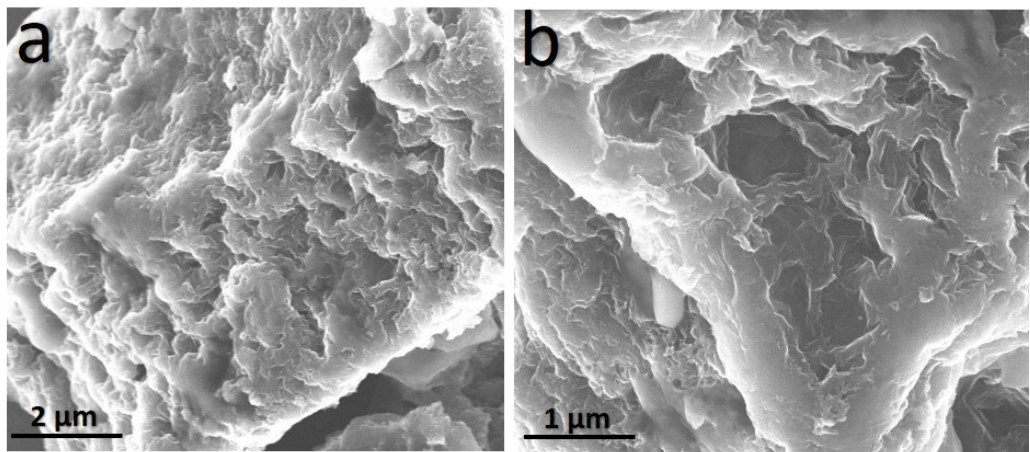


**Figure S1:** FESEM images of 3DNSrGO

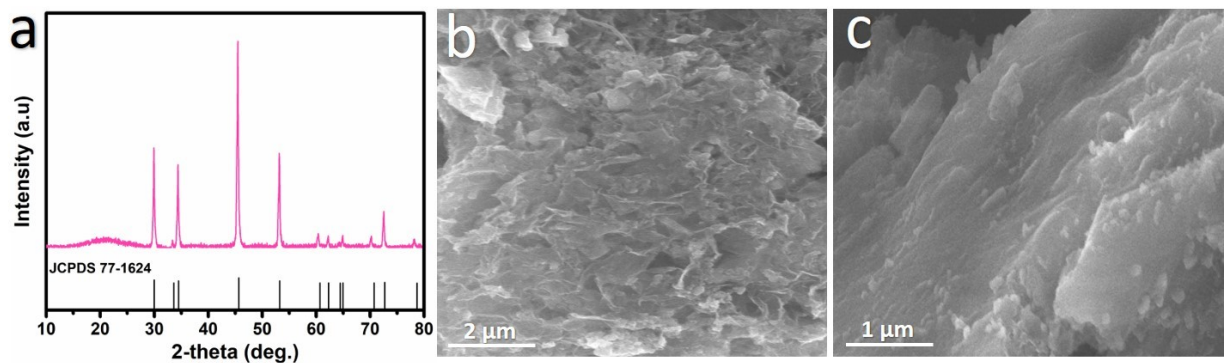


**Figure S2:** (a) XRD pattern, (b-c) FESEM images of NiS/NSrGO without PVP.

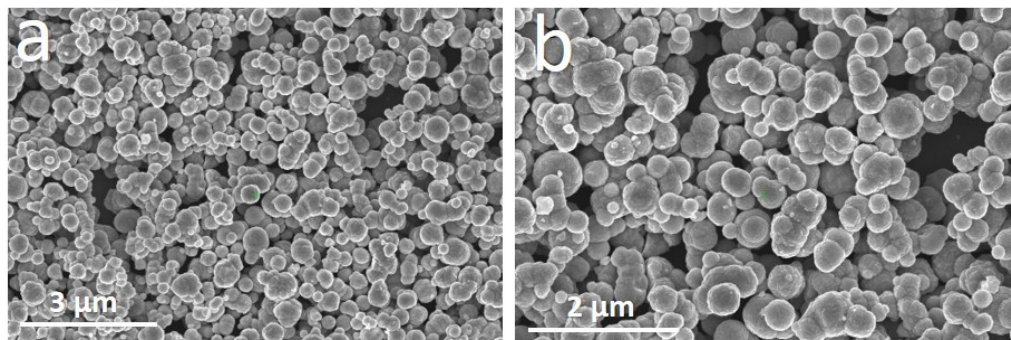


**Figure S3:** FESEM images of NiS particles.

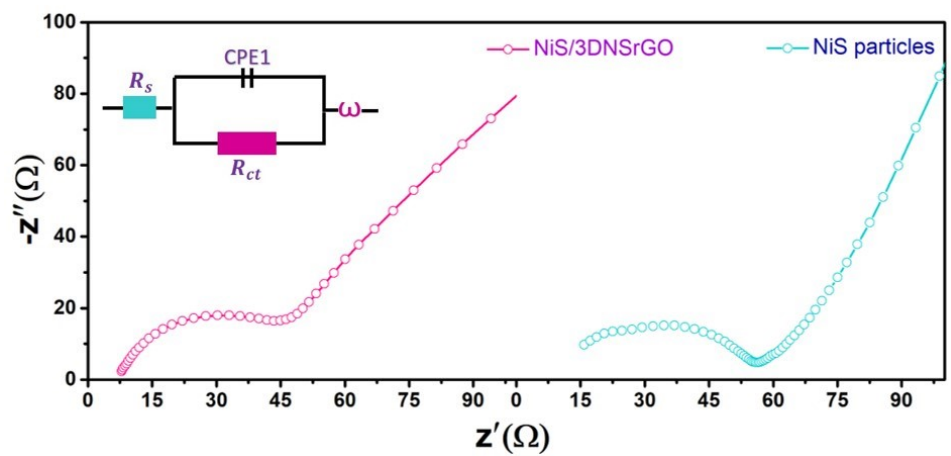


**Figure S4:** Electrochemical Impedance Spectroscopy tested before cycling for NiS/3DNSrGO and NiS particles.

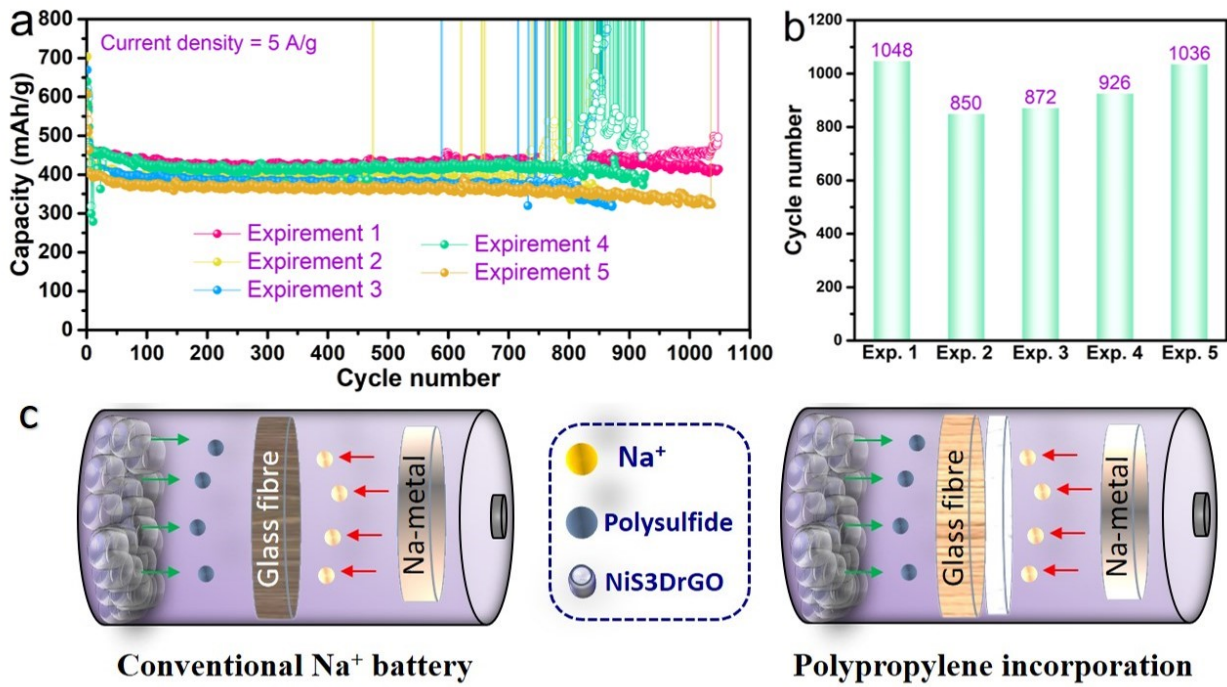


**Figure S5:** (a) Comparative study of NiS/3DNSrGO cell failure without propylene membrane (b) Evaluation of cycle life across the repeated experiments (c) Schematic representation of SIB.

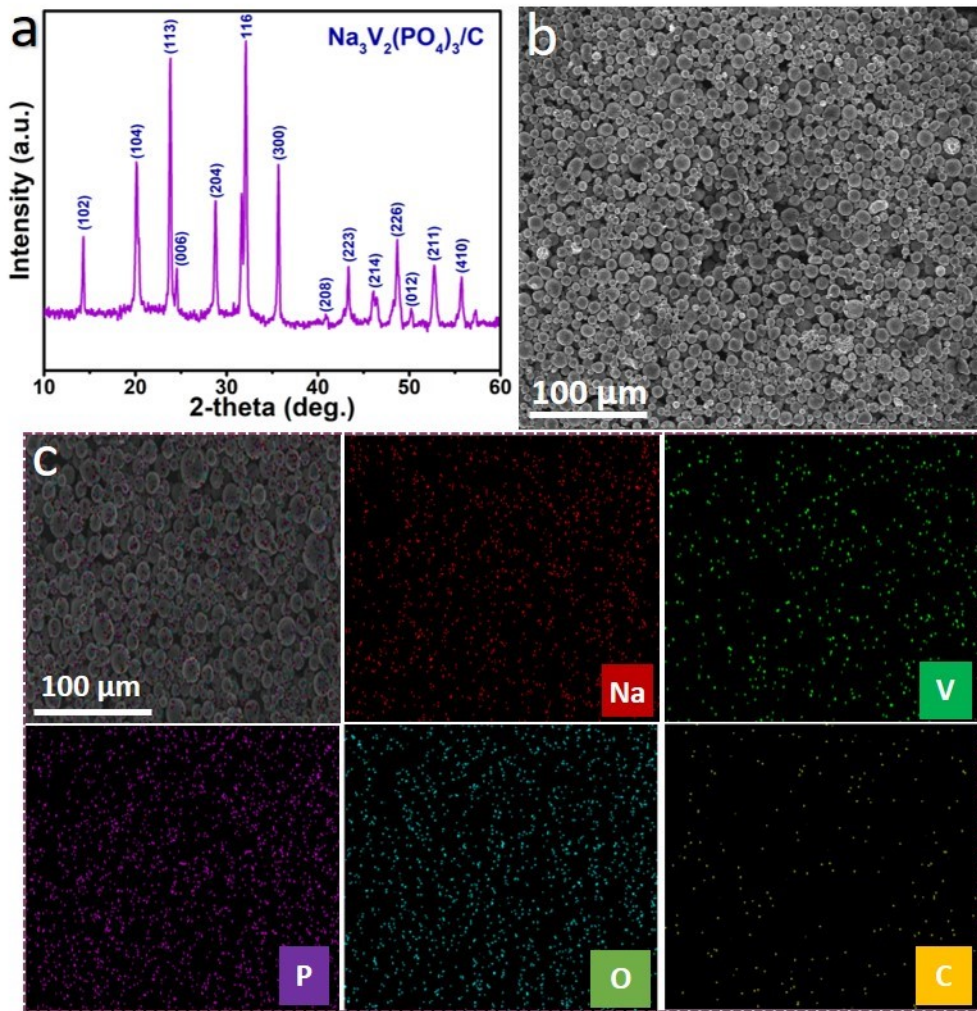


**Figure S6:** (a) XRD (b) FESEM image (c) EDX mapping of the  $\text{Na}_3\text{V}_2(\text{PO}_4)_3/\text{C}$  cathode.

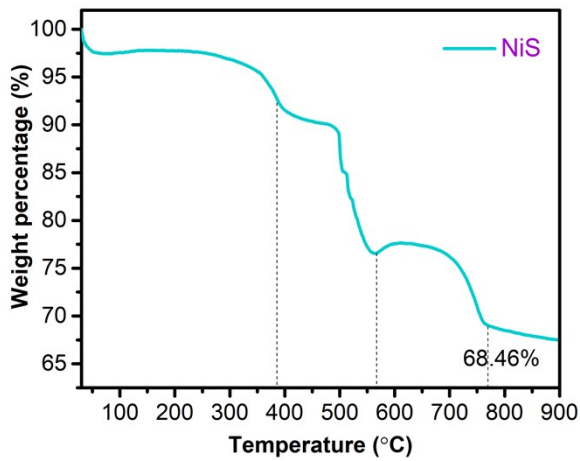


**Figure S7:** Thermogravimetric analysis (TGA) of NiS particles.

The weight loss observed below 400 °C can be attributed to the removal of adsorbed moisture and after 500 °C is primarily due to the thermal decomposition of NiS, releasing sulfur in the form of gaseous species (SO<sub>2</sub>, S, etc.). Furthermore, weight loss around 700 °C is likely associated with the complete decomposition of NiS, and any remaining sulfur is released as gas.

Carbon content calculation:

Sample	Weight percentage at 900°C	Wight difference with and without NSrGO
NiS	68.46%	
NiS+NSrGO	49.10%	19.36%

Considering NiS and NiS/NSrGO samples under the O<sub>2</sub> pyrolysis process, NiS will be converted into solid oxide compounds such as NiO and Ni<sub>3</sub>O<sub>4</sub> and volatile compounds (SO<sub>2</sub>). Therefore, 100% NiS can produce a 68.46% weight loss according to the TGA results. For NiS/NSrGO, with a set content of NiS at  $x\%$ , the carbon content is  $(100 - x)\%$ . This composite will be converted into solid oxides (NiO, Ni<sub>3</sub>O<sub>4</sub>, etc.) and volatile SO<sub>2</sub> and CO<sub>2</sub>. Thus,  $x\%$  NiS/NSrGO can produce a 49.10% weight loss according to the TGA results. From  $\frac{100}{68.46} = \frac{x}{49.10}$ , Consequently,  $x = 71.72\%$ , and therefore the carbon content is 28.3%.

**Table S1:** Corresponding rate performances of NiS/3DNSrGO electrode.

<b>Current Density (A/g)</b>	<b>Specific Capacity (mAh/g)</b>	<b>Cycle number</b>
0.1	572	1-10
0.2	497	11-20
0.5	471	21-30
1.0	449	31-40
2.0	428	41-50
5.0	383	51-60
10	359	61-70

**Table S2:** Corresponding rate performances of NiS/3DNSrGO+PP electrode.

<b>Current Density (A/g)</b>	<b>Specific Capacity (mAh/g)</b>	<b>Cycle number</b>
0.1	587	1-10
0.2	528	11-20
0.5	499	21-30
1.0	479	31-40
2.0	458	41-50
5.0	421	51-60
10	386	61-70

**Table S3.** Comparison of our material with some transition metal/graphene-based materials in terms of rate performance and cycle durability.

Material	Capacity/Current density	Cycle Life	Rate capability	Ref.
<i>NiS/3DNiSrGO</i>	405 mAh/g (5 A/g)	2000 Cycles	386 mAh/g (10 A/g)	This work
<i>NiS<sub>1.03</sub>/S-rGO</i>	242.1 mAh/g (0.5 A/g)	200 cycles	251.7 mAh/g (4 A/g)	1
<i>NbSSe/CN</i>	347.8 mAh/g (1 A/g)	1000 Cycles	262.4 mAh/g (5 A/g)	2
<i>NiS<sub>1-x</sub>Se<sub>x</sub>@N-rGO</i>	300 mAh/g (1 A/g)	1000 Cycles	398 mAh/g (5 A/g)	3
<i>MoS<sub>1.2</sub>Se<sub>0.8</sub>/G</i>	178 mAh/g (2 A/g)	700 Cycles	140 mAh/g (5 A/g)	4
<i>MoS<sub>1.5</sub>Te<sub>0.5</sub>@C</i>	355.4 mAh/g (1 A/g)	500 Cycles	352.3 mAh/g (5 A/g)	5
<i>Ni<sub>3</sub>S<sub>2</sub>/GO</i>	76.3 mAh/g (5 A/g)	500 Cycles	115.2 mAh/g (5 A/g)	6
<i>NiS@C/rGO</i>	240.2 mAh/g (0.1 A/g)	500 Cycles	324.1 mAh/g (1 A/g)	7
<i>Cu<sub>2</sub>S/MoS<sub>2</sub>@PCF</i>	245.2 mAh/g (4 A/g)	800 Cycles	260.2 mAh/g (10 A/g)	8
<i>US-MoS<sub>2</sub>@NG</i>	198 mAh g <sup>-1</sup> (1A/g)	1000 Cycles	141 mAh/g (12.8 A/g)	9
<i>FeS<sub>2</sub>-C/RG</i>	291.7 mAh/g (6A/g)	1000 Cycles	-	10
<i>C@MoS<sub>2</sub>@PPy</i>	294 mAh/g (5 A/g)	500 Cycles	417 mAh/g (2 A/g)	11
<i>NiS<sub>2</sub>/N,S-rGO</i>	207.7 mAh/g (0.1 A/g)	200 Cycles	205.1 mAh/g (1 A/g)	12
<i>NiS<sub>2</sub>/rGO</i>	308 mAh/g (5 A/g)	500 Cycles	302 mAh/g (10 A/g)	13

<b>NiS/SnS@NC</b>	412 mAh/g (2A/g)	500 Cycles	396 mAh/g (5 A/g)	14
<b>SnS<sub>2</sub>/NiS<sub>2</sub>@S-rGO</b>	340.7 mAh/g (5 A/g)	2200 Cycles	383.5 mAh/g (5 A/g)	15
<b>CoS<sub>2</sub>@rGO+PP</b>	398 mAh/g (5A/g)	1000 Cycles	-	16
<b>CoTe<sub>2</sub>@3DG</b>	103 mAh/g (1A/g)	4500 Cycles	135 mAh/g (5A/g)	17
<b>Co<sub>4</sub>S<sub>3</sub>@NSC/MoS<sub>3</sub></b>	435 mAh/g (2A/g)	600 Cycles	382 mAh/g (10A/g)	18

## Supplementary References

1. J. Li, Z. Ding, J. Li, C. Wang, L. Pan, G. Wang, Synergistic coupling of NiS<sub>1.03</sub> nanoparticle with S-doped reduced graphene oxide for enhanced lithium and sodium storage, Chemical Engineering Journal, 407 (2021) 127199.
2. Y. Liu, M. Qiu, X. Hu, J. Yuan, W. Liao, L. Sheng, Y. Chen, Y. Wu, H. Zhan, Z. Wen, Anion Defects Engineering of Ternary Nb-Based Chalcogenide Anodes Toward High-Performance Sodium-Based Dual-Ion Batteries, Nano-Micro Letters, 15 (2023) 104.
3. S. Zhang, R. Wang, R. Cao, F. Fang, R. Wu, NiS<sub>1-x</sub>Sex Nanoparticles Anchored on Nitrogen-Doped Reduced Graphene Oxide as Highly Stable Anode for Sodium-Ion Battery, Processes, 2022.
4. Y. Zhang, H. Tao, S. Du, X. Yang, Conversion of MoS<sub>2</sub> to a Ternary MoS<sub>2-x</sub>Sex Alloy for High-Performance Sodium-Ion Batteries, ACS Applied Materials & Interfaces, 11 (2019) 11327-11337.
5. Y. Liu, X. Hu, J. Li, G. Zhong, J. Yuan, H. Zhan, Y. Tang, Z. Wen, Carbon-coated MoS<sub>1.5</sub>Te<sub>0.5</sub> nanocables for efficient sodium-ion storage in non-aqueous dual-ion batteries, Nature Communications, 13 (2022) 663.
6. Y.-h. Zhang, R.-h. Liu, L.-j. Xu, L.-j. Zhao, S.-h. Luo, Q. Wang, X. Liu, One-pot synthesis of small-sized Ni<sub>3</sub>S<sub>2</sub> nanoparticles deposited on graphene oxide as composite anode materials for high-performance lithium-/sodium-ion batteries, Applied Surface Science, 531 (2020) 147316.

7. Z. Song, G. Wang, Y. Chen, Q. Chang, Y. Lu, Z. Wen, Construction of hierarchical NiS@C/rGO heterostructures for enhanced sodium storage, *Chemical Engineering Journal*, 435 (2022) 134633.
8. N. Shi, B. Xi, M. Huang, X. Ma, H. Li, J. Feng, S. Xiong, Hierarchical Octahedra Constructed by Cu<sub>2</sub>S/MoS<sub>2</sub>Carbon Framework with Enhanced Sodium Storage, *Small*, 16 (2020) 2000952.
9. X. Xu, R. Zhao, W. Ai, B. Chen, H. Du, L. Wu, H. Zhang, W. Huang, T. Yu, Controllable Design of MoS<sub>2</sub> Nanosheets Anchored on Nitrogen-Doped Graphene: Toward Fast Sodium Storage by Tunable Pseudocapacitance, *Advanced Materials*, 30 (2018) 1800658.
10. F. Wang, W. Zhang, H. Zhou, H. Chen, Z. Huang, Z. Yan, R. Jiang, C. Wang, Z. Tan, Y. Kuang, Preparation of porous FeS<sub>2</sub>-C/RG composite for sodium ion batteries, *Chemical Engineering Journal*, 380 (2020) 122549.
11. G. Wang, X. Bi, H. Yue, R. Jin, Q. Wang, S. Gao, J. Lu, Sacrificial template synthesis of hollow C@MoS<sub>2</sub>@PPy nanocomposites as anodes for enhanced sodium storage performance, *Nano Energy*, 60 (2019) 362-370.
12. X. Dong, F. Chen, G. Chen, B. Wang, X. Tian, X. Yan, Y.-X. Yin, C. Deng, D. Wang, J. Mao, S. Xu, S. Zhang, NiS<sub>2</sub> nanodots on N,S-doped graphene synthesized via interlayer confinement for enhanced lithium-/sodium-ion storage, *Journal of Colloid and Interface Science*, 619 (2022) 359-368.
13. H. Zheng, X. Chen, L. Li, C. Feng, S. Wang, Synthesis of NiS<sub>2</sub>/reduced graphene oxide nanocomposites as anodes materials for high-performance Sodium and Potassium ion batteries, *Materials Research Bulletin*, 142 (2021) 111430.
14. B. Yan, L. Lin, H. Sun, T. Zhang, C. Xu, C. Sun, L. Zhang, X. Yang, Double-shelled NiS/SnS@N-doped carbon nanoboxes engineered from NiSn(OH)<sub>6</sub> cube templates for advanced sodium-ion battery anodes, *Chemical Engineering Journal*, 477 (2023) 146950.
15. H. Li, Y. He, Y. Dai, Y. Ren, T. Gao, G. Zhou, Bimetallic SnS<sub>2</sub>/NiS<sub>2</sub>@S-rGO nanocomposite with hierarchical flower-like architecture for superior high rate and ultra-stable half/full sodium-ion batteries, *Chemical Engineering Journal*, 427 (2022) 131784.
16. T. Li, B. Wang, H. Song, P. Mei, J. Hu, M. Zhang, G. Chen, D. Yan, D. Zhang, S. Huang, Deciphering the Performance Enhancement, Cell Failure Mechanism, and Amelioration Strategy of Sodium Storage in Metal Chalcogenides-Based Andes, *Advanced Materials*, n/a (2024) 2314271.

17. Y. Jiang, F. Wu, Z. Ye, Y. Zhou, Y. Chen, Y. Zhang, Z. Lv, L. Li, M. Xie, R. Chen, Superimposed effect of hollow carbon polyhedron and interconnected graphene network to achieve CoTe<sub>2</sub> anode for fast and ultralong sodium storage, *Journal of Power Sources*, 554 (2023) 232174.
18. J. Yan, K. Sang, X. Jiang, Q. Li, F. Jiang, Y. Zhou, Amorphous MoS<sub>3</sub>-modified porous Co<sub>4</sub>S<sub>3</sub>-embedded N,S co-doped carbon polyhedron as new high-capacity and high-rate anode materials for sodium-ion half/full cells, *Journal of Colloid and Interface Science*, 655 (2024) 100-109.